Test beam 2003
Short status of data analysis

P. Ronchese, S. Vanini and P. Zotto
(Dip. di Fisica dell'Università and sez. INFN di Padova)

July 26th, 2003

Abstract

A first round of data analysis was performed on the data collected during the 2003 test beam. Very preliminary results on efficiency and basic performance of the trigger system are reported.

1. Introduction

The 2003 test beam featured a run using a 40 MHz bunched beam. The most important result was the proof that the integration of the several different devices lodged on the minicrate was done adequately both on the hardware and software side of the system. Furthermore the test was done in order to provide complete information about the general performance of the trigger algorithms. The data used in this analysis were only the ones collected with the default configuration setup at various incident angles. This setup is the one currently proposed for the data taking at LHC and it is the basis of all the predictions of the trigger performance. A first order comparison with the current trigger emulator performance is attempted. A limited amount of data (50000 events per run) was used.

2. Data selection

The selection of the data was done trying to avoid any possible bias on the trigger performance evaluation. Since the triggering device was a scintillator, the main request is the presence of its signal, whose time was recorded from the chamber TDCs. The tolerance on this signal was put to two nanoseconds. The other request was the existence of recorded signals within a 500 ns window on at least two cells in the region illuminated from the beam, in order to reject beam halo triggers. The overall rejected fraction of events was around 0.5 %. The trigger data were recorded inside a pattern unit storing information at 40 Mhz. The pattern unit was started from the scintillator signal and data available in the first 40 locations (slots) were readout.

3. Timing response

The system is designed to give a late trigger upon detection of the alignment of hits in staggered drift tubes planes making use of the drift time information (BTI devices). Further stages of the system are used to correlate between independent candidates in both superlayers (TRACO devices) and to select the best candidates among all the ones in a chamber (TS system).

The system is rather noisy since, requiring a minimum of three aligned hits to gain in efficiency, many false alignments are detected and therefore a certain temporal spectra of ghost triggers accompanying the correct one is expected. The spectra obtained for few cases are reported in Figure 1 where the pattern unit slot of the recorded trigger is showed for some relevant incidence angles (normal, close to maximum, average positive and average negative angles) separated for trigger types. Label H identifies BTI alignments of four hits, while label L marks BTI alignments of three hits. In addition the first three triggers types of each row are TRACO successful correlation of H or L candidates in the inner and outer superlayers, while the other four are uncorrelated trigger of either the inner or the outer SL as identified from the subscript.

The cleanest trigger types are HH and HL triggers that immediately permits the evaluation of output clock 14 as the right one, thus classifying the triggers in the other locations as ghost triggers (remind that this clock is relative to pattern unit startup time). Most of these false triggers are included in the uncorrelated category with a non negligible fraction of correlated LL triggers. Some noise reduction in the uncorrelated L category is applied in the default configuration and a full understanding of noise triggers will be available only after control of the effect of each noise suppression mechanism as activated in the non-default configurations.

Within each chamber the trigger system provides up to two candidate tracks per clock in order to allow multimuon detection and as a recovery mechanism in case the best choice selects a ghost track. The second track is marked and transmitted one clock after the first track if no other first track was found. The time spectra for first and second tracks is shown in Figure 2 where the same conclusion about ghost tracks can be obtained. Notice that the correct output clock of second tracks is 15 (i.e. one clock later than good first tracks). The fraction of events with a second track is ranging from about 7% to 14 %.

4. Efficiency

The overall efficiency is obtained counting triggers occurring at the correct clock. The efficiency computed in this way can be called bunch crossing efficiency, since no attempt is made to check if the output parameters correspond to the actual muon track parameters. The only way to make a more sophisticate efficiency determination is to have an external device that could provide independently position and direction of the detected muons: using the parameters computed from the track fit algorithm is misleading, because the trigger algorithm is essentially performing a rough track fit using the same input data.

The bunch crossing efficiency is shown in Figure 3 as a function of the angle comparing it to the result of the current emulation algorithm. The result is good, since the efficiency is almost flat in the range 98-99% up to ~35°: the small drop at normal incidence is due to tracks hitting two I-beams in both the superlayers. The emulator result is statistically satisfactory since a relevant difference is found only at very large inclination

A deeper insight on the algorithm performance both hardwarewise and in its emulator form can be obtained checking the fraction of trigger types as a function of the angle. The contribution to the efficiency of each trigger type is shown in Figure 4 grouping correlated and uncorrelated triggers and in Figure 5 splitting up for any kind of trigger.

There is evidence of a progressive reduction of the correlated triggers with increasing inclination, and of their fast drop at very large angle where most of the triggers are uncorrelated.

Figure 6 and Figure 7 show a comparison between hardware and emulator results, showing a deficit (~8%) of HH trigger in the emulator (compensated by a roughly equal number of HL triggers) and a too large amount of second tracks generated in the emulator with respect to the actual trigger results.

As expected the relative amount of uncorrelated triggers is much larger in the second track selection.

5. Correlations

The output trigger parameters are the radial angle (corresponding to the position where the muon is crossing the chamber expressed in polar coordinates) and the bending angle (corresponding to the deviation from radial direction of the vector crossing the chamber). The first parameter can be directly compared to the position measured from the track fit, while the second one can be transformed in the incidence angle, since there is no bending due to magnetic field and therefore it is just an artefact of the geometrical layout.

In both cases a certain care must be taken, since the evaluation of the crossing point is done in different positions depending on the trigger type (at chamber center for correlated tracks and at the center of inner or outer superlayers respectively for inner or outer uncorrelated triggers). Instead the offline track fit is evaluated in yet another different point: the comparison needs therefore an extrapolation of the fitted track to the actual planes used in the calculation of the TRACO look up tables.

Figure 8 shows the correlation between muon crossing position and radial angle for real data and emulator at 0˚. The distributions of correlated, uncorrelated inner and uncorrelated outer triggers are reported in the same plot. In this case the effect of the different evaluation planes is negligible. Therefore the gap of the order of 1 cm among the triggers classified in these different classes can be attributed to an error in the LUTs calculation. Another effect is a step in the lines that are in fact not continuos: this step exactly corresponds to the border between TRACO 9 and TRACO 10 and again can be attributed to a problem in the calculation. The same problem does not appear in the emulator plot and could be associated to the fact that the calculations are done independently on different machines (a PC and a microcontroller) and with different languages (C++ and C): a cross check between the two codes must be done.

The extrapolation is instead necessary to allow any discussion about the quality of correlation at different incident angles. Figures 9-12 show that once correcting for this effect the correlation lines are essentially the same at any inclination.

The incident angle can be computed using radial and bending angle and it can be compared to the same angle as measured for the fitted track inclination. This comparison is done in the plot of Figure 13 that shows a nice correlation between the two quantities.

6. Conclusions

The trigger performance seems to be rather good and close to the expected design goals. Sensible explanations for most of the observed strange behaviours could be found although some problems arised during this analysis need further work.

The software emulator default flow has some deviations from the hardware results, but its behaviour is close enough to them to let us believe that the performance foreseen for the muon local drift tube trigger in CMS can be statistically correct.

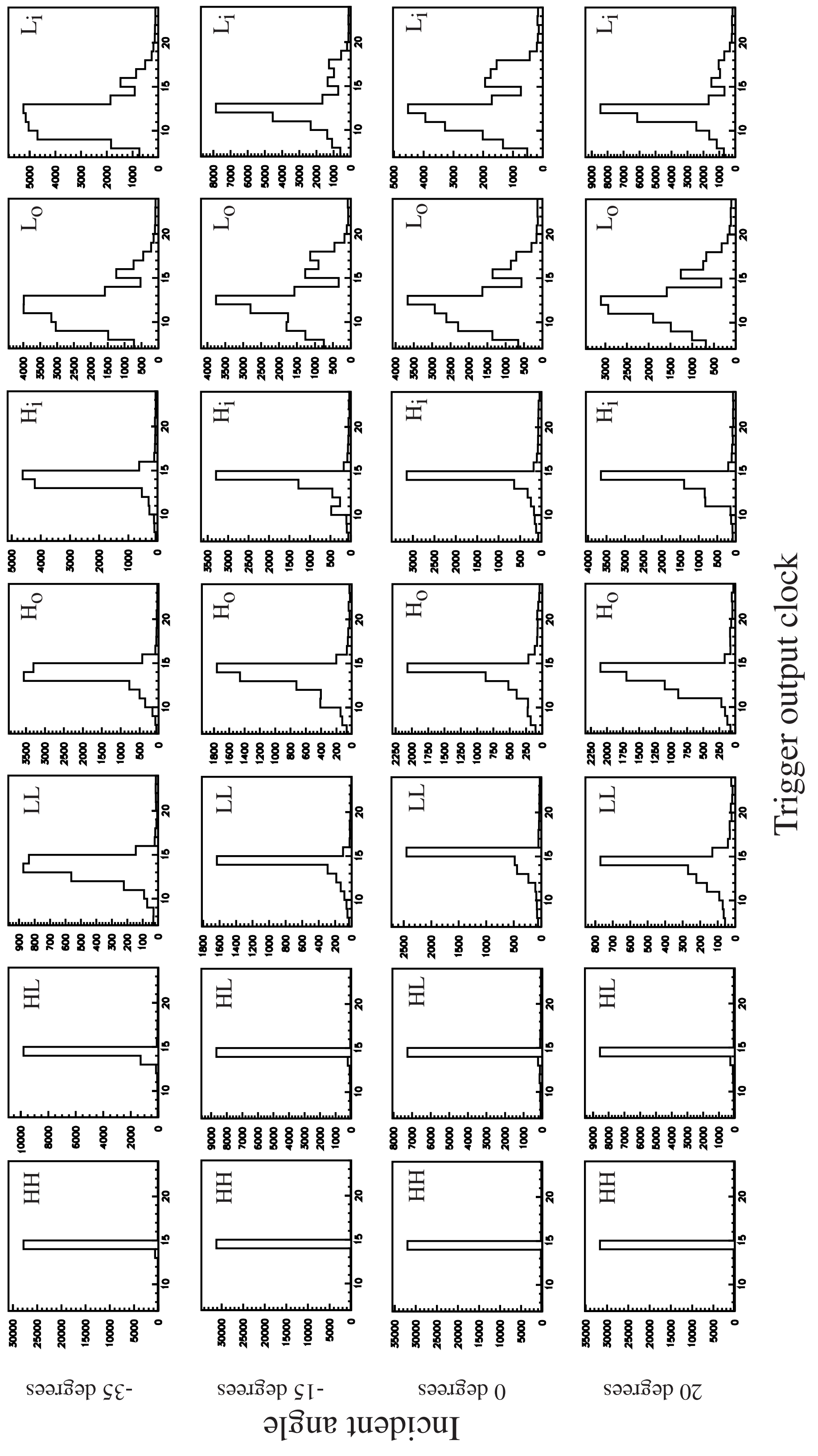

Figure 1- Pattern unit recorded slot for different trigger types at several incident angles

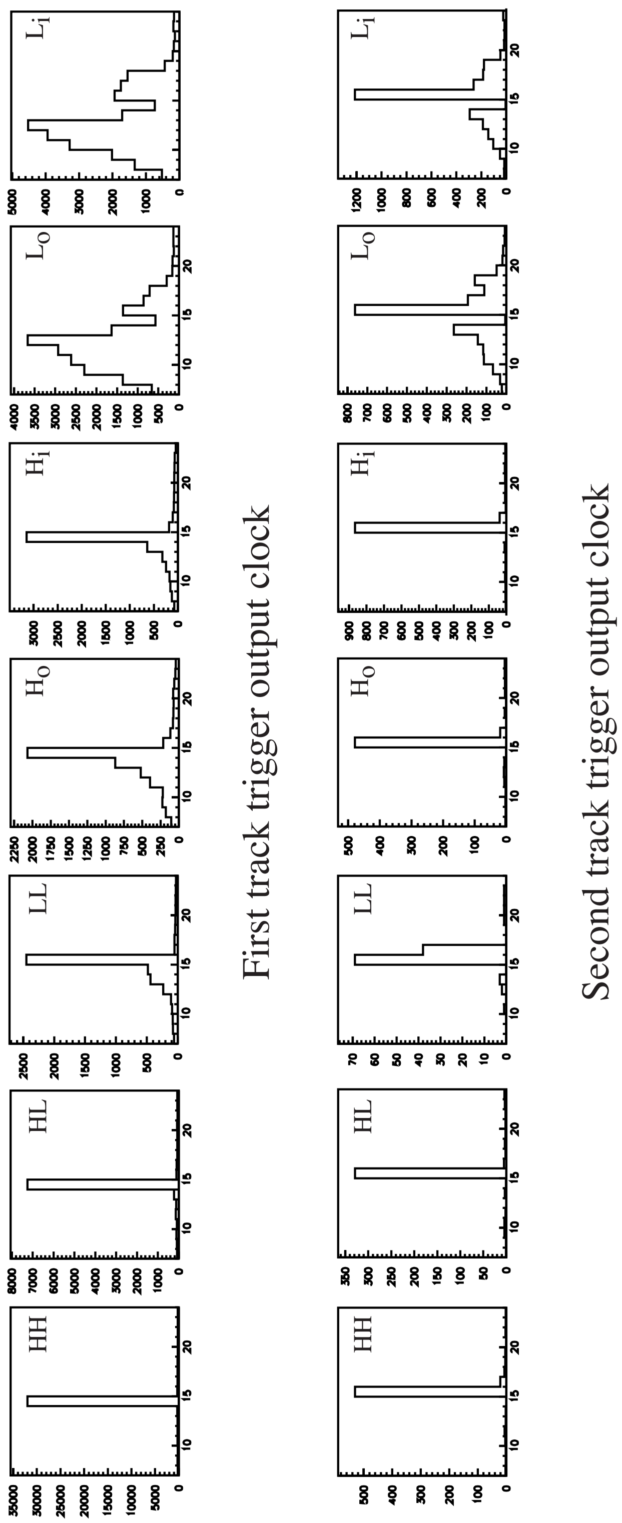

Figure 2- Pattern unit slot for different trigger types divided between first and second track

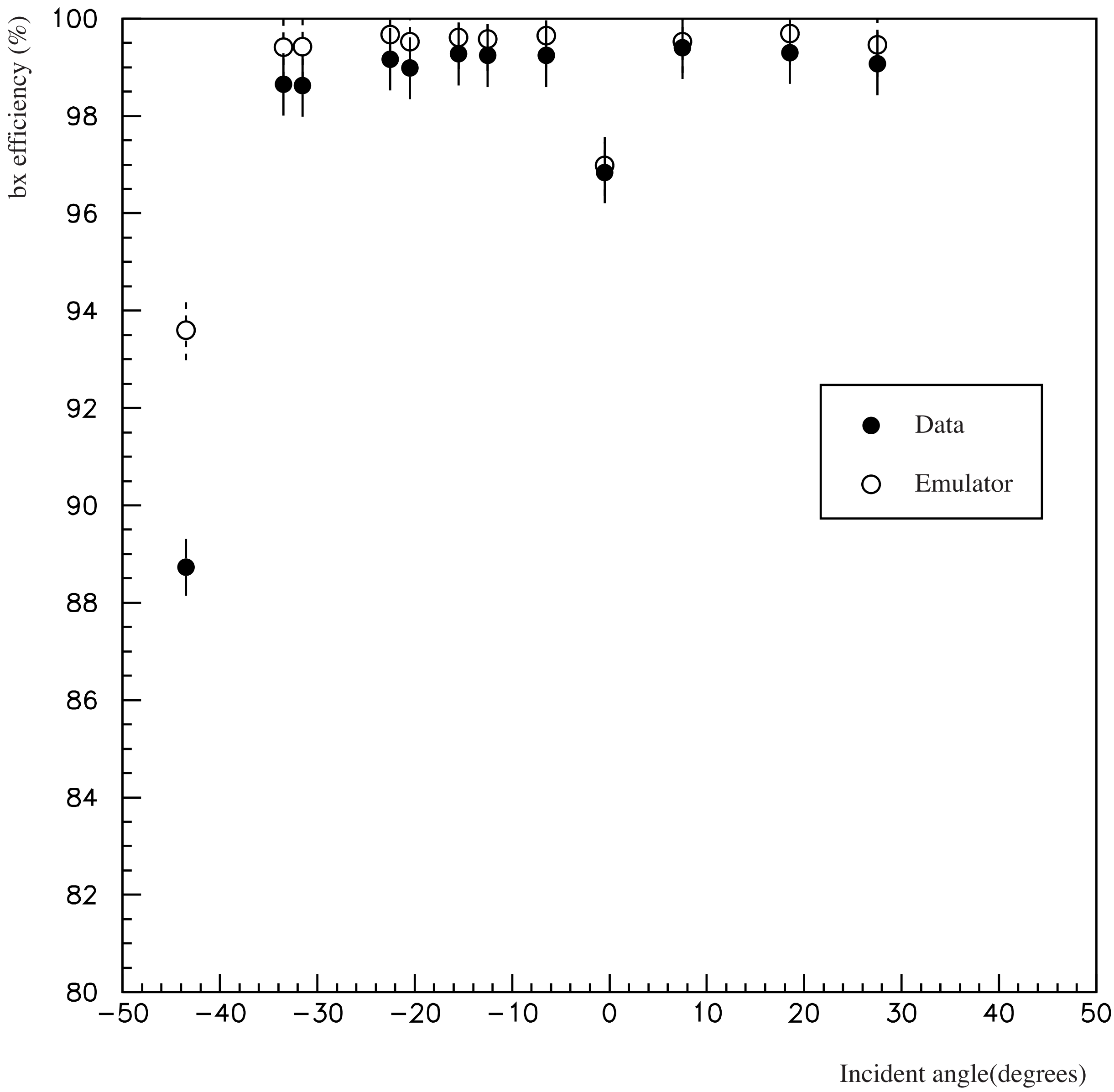

Figure 3- Bunch crossing efficiency as a function of the angle of incidence. Data are compared to emulator results based on the same input drift times.

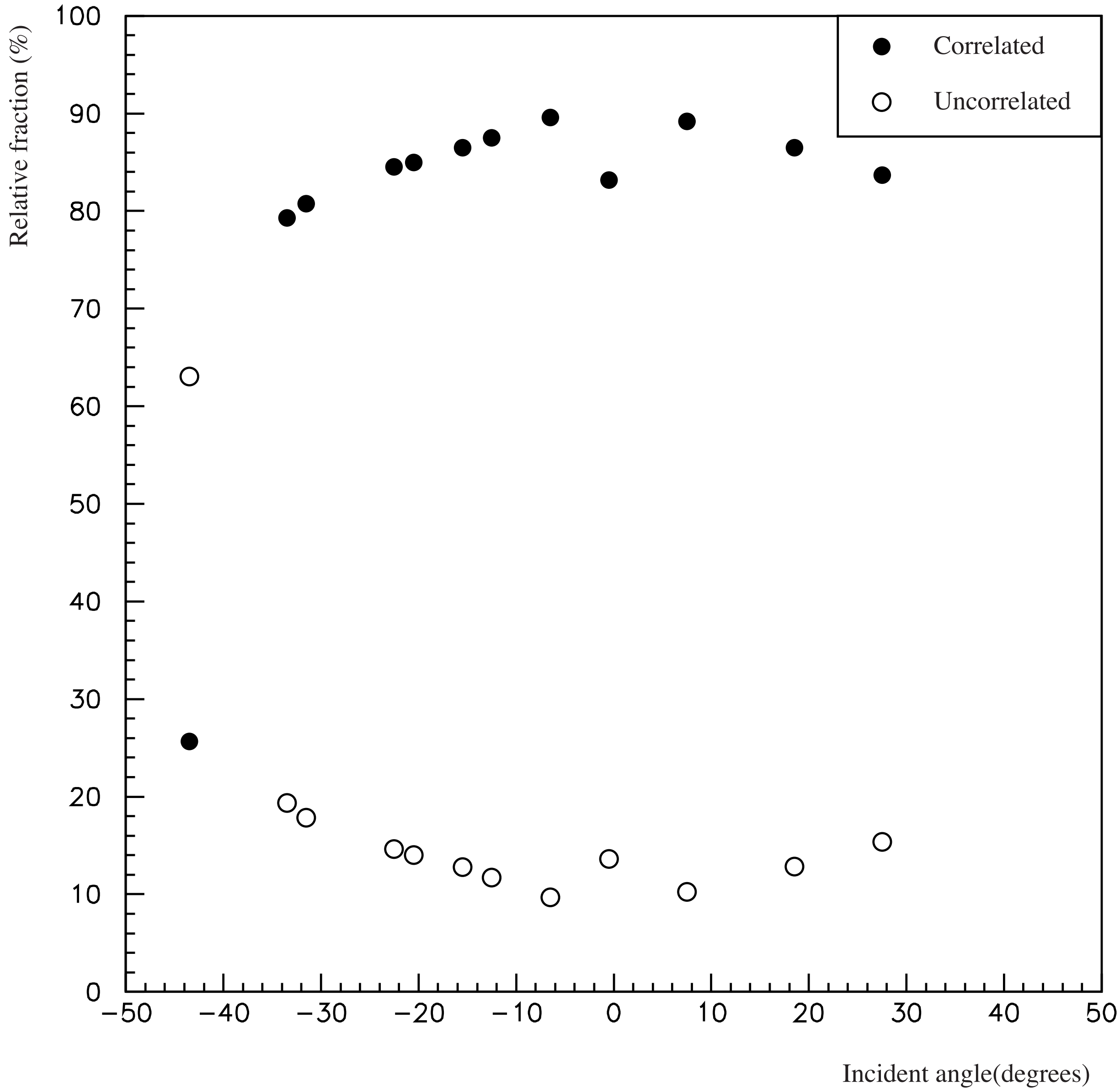

Figure 4- Contribution to the bunch crossing efficiency of correlated and uncorrelated triggers

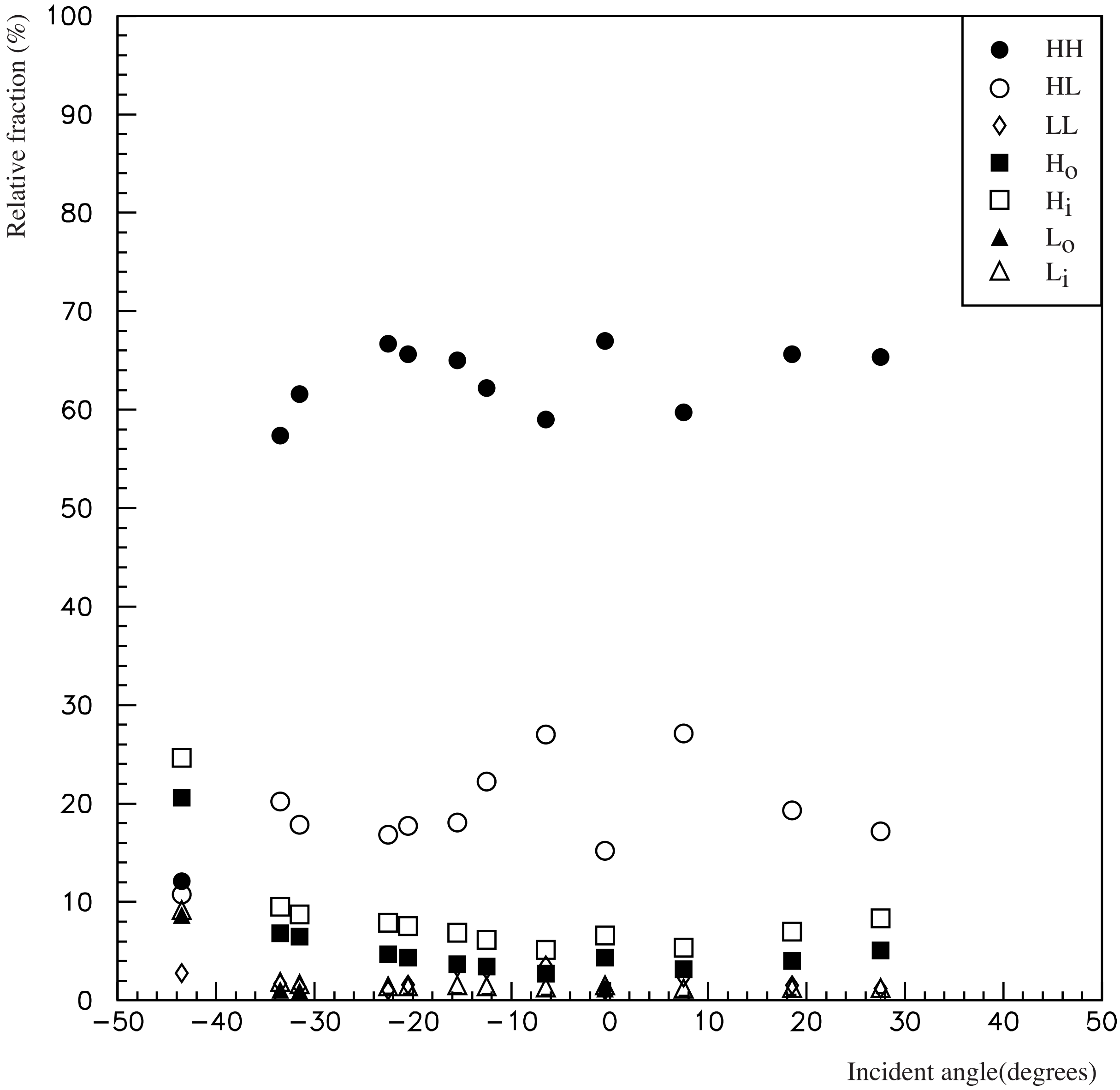

Figure 5- Relative contribution to bunch crossing efficiency of any trigger type

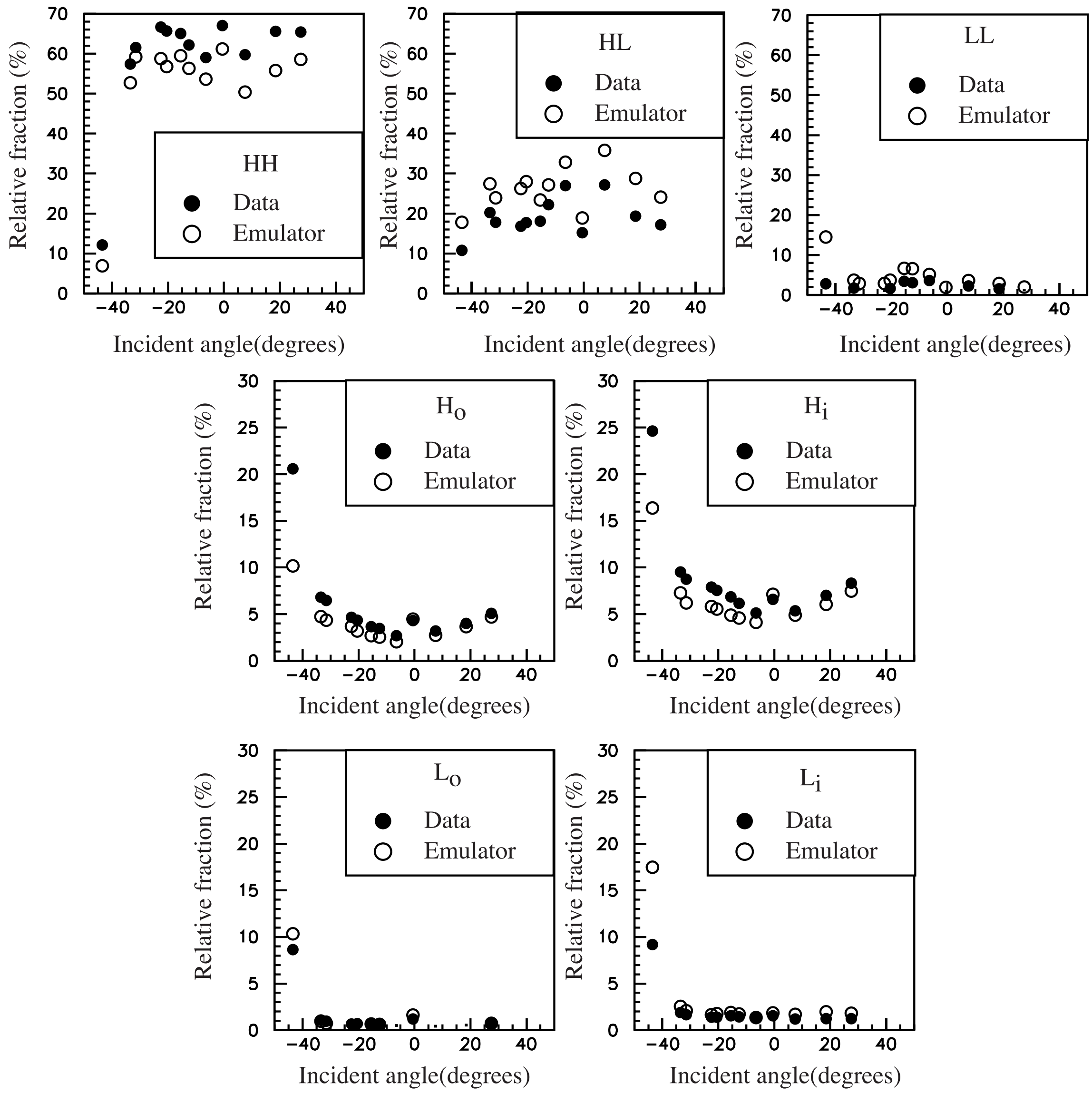

Figure 6- Relative contribution of each trigger type as a function of incident angle compared to emulator results

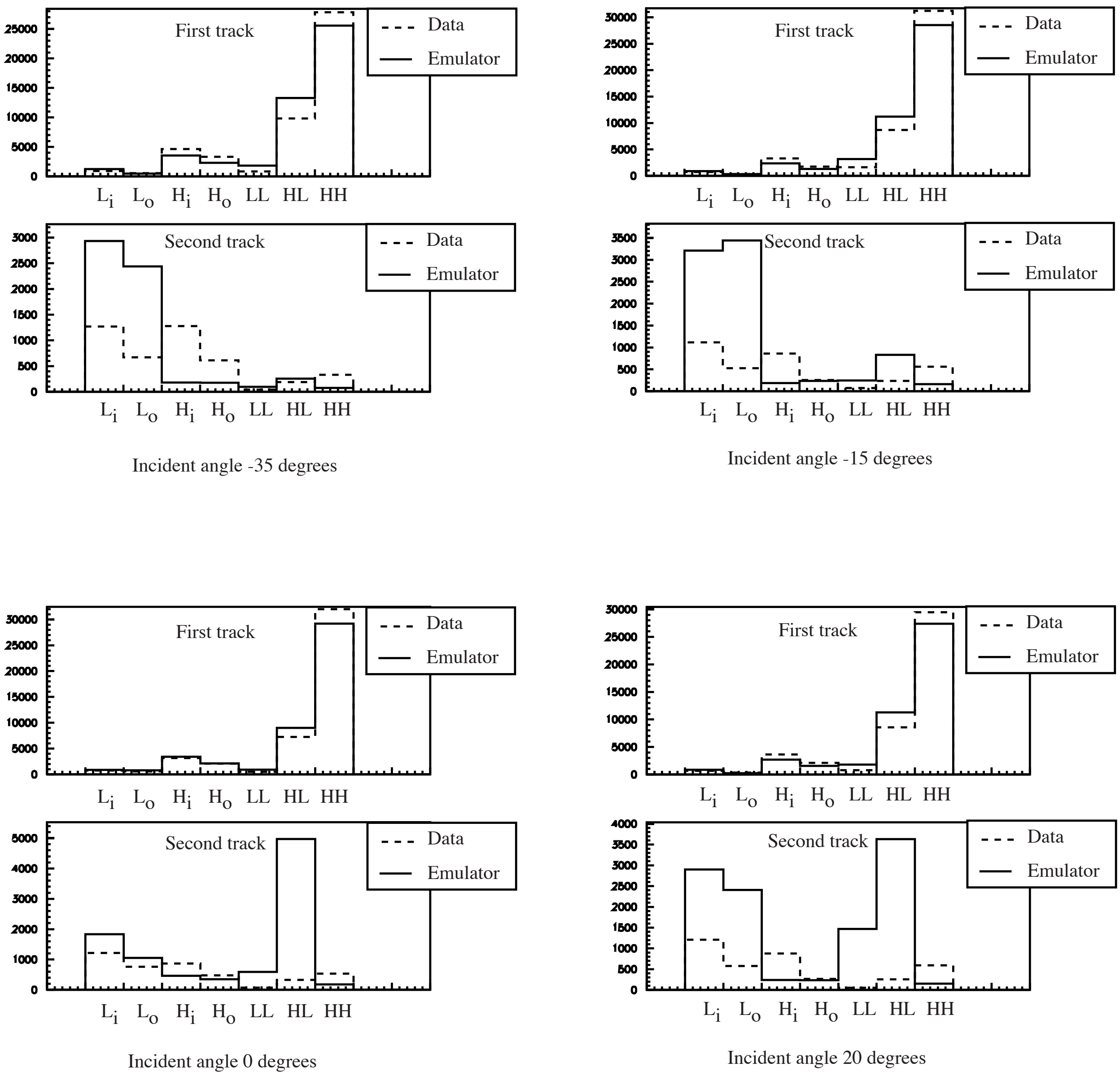

Figure 7- Comparison of emulator results and actual triggers for few incidence angles. Results are compared for all the different trigger types and first and second track separately.

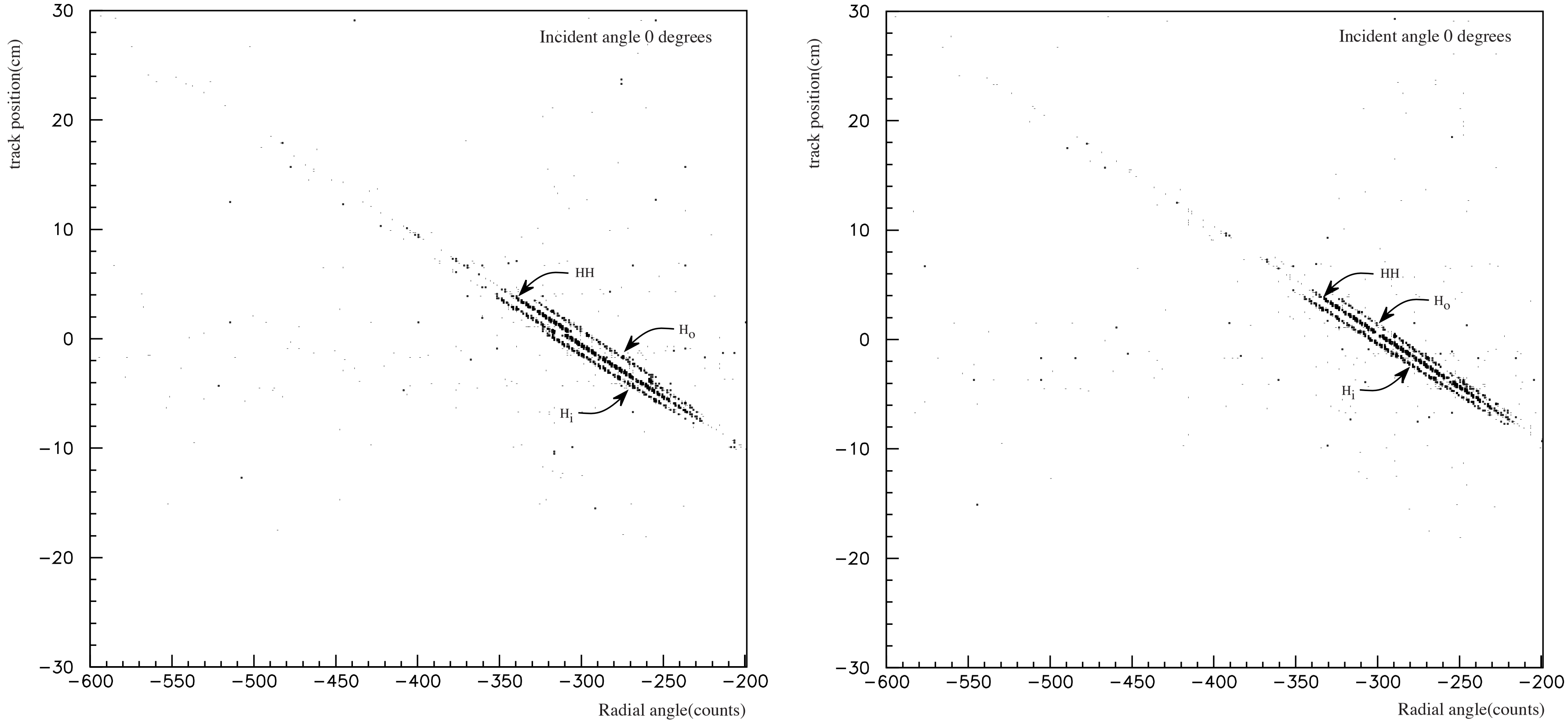

Figure 8- Correlation between crossing coordinate measured from a track fit and radial angle as output from the trigger at correct clock for emulator (right) and beam test (left).

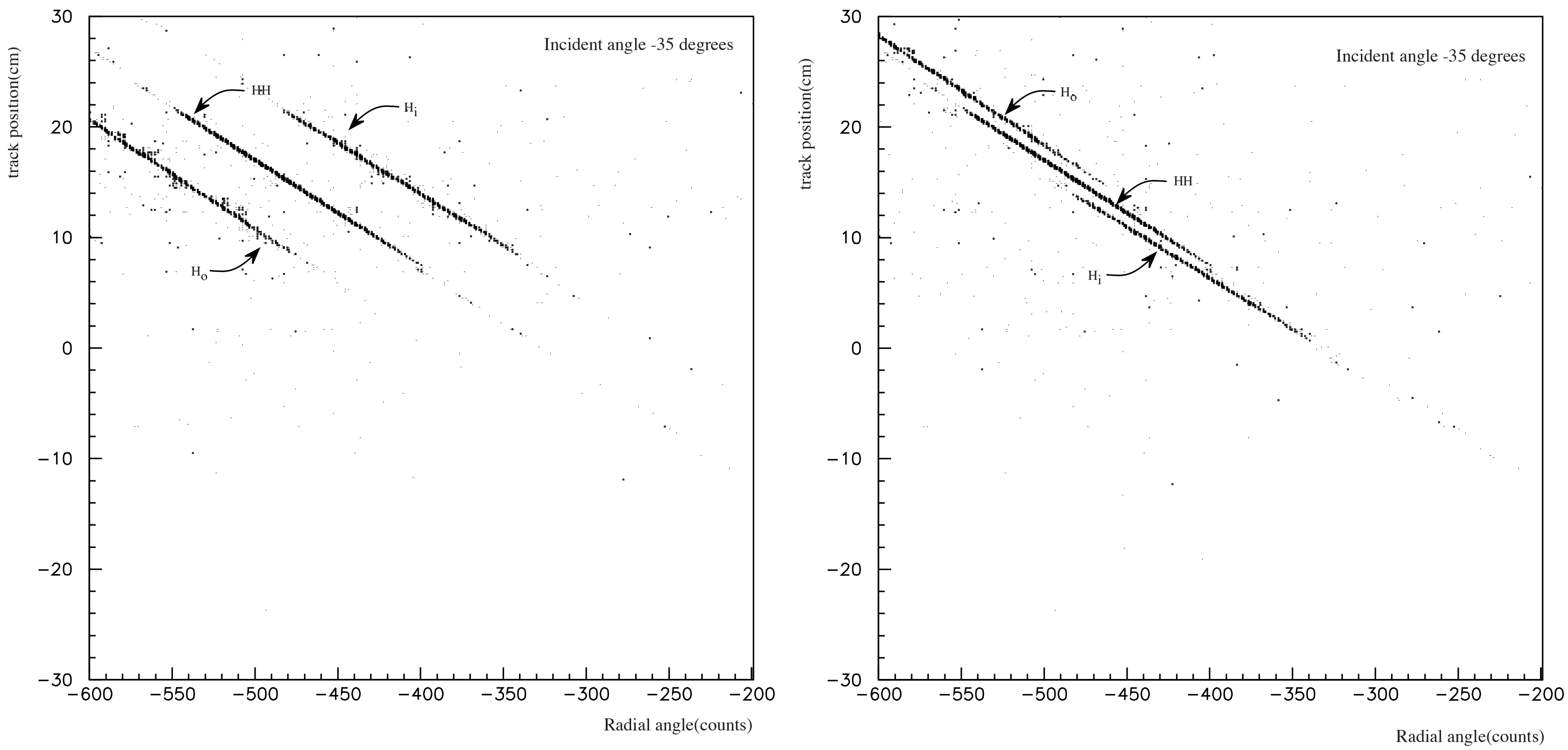

Figure 9- Correlation between crossing coordinate measured from a track fit and radial angle as output from the trigger at correct clock before extrapolation (left) and after extrapolation (right.)

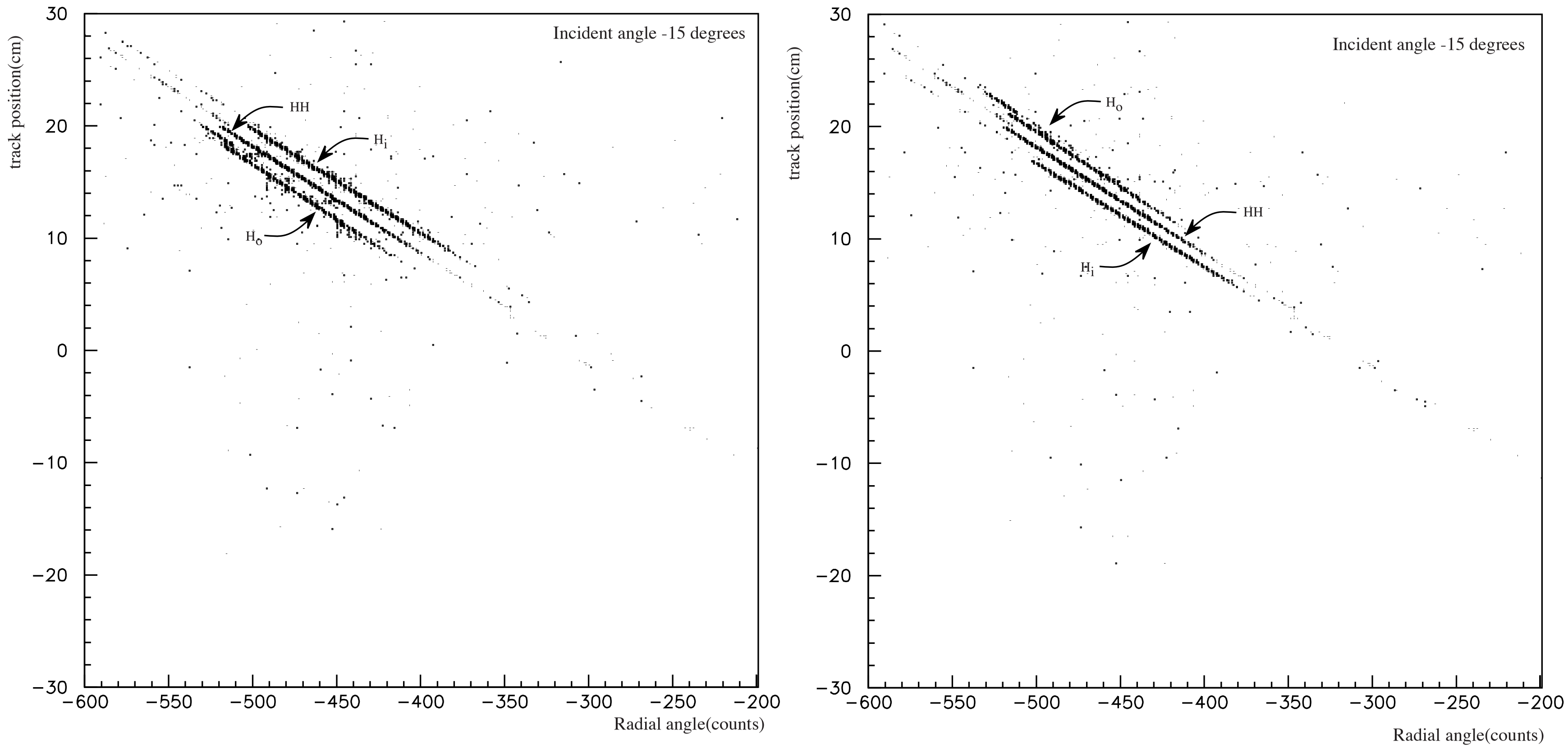

Figure 10- Correlation between crossing coordinate measured from a track fit and radial angle as output from the trigger at correct clock for emulator before extrapolation (left) and after extrapolation (right.

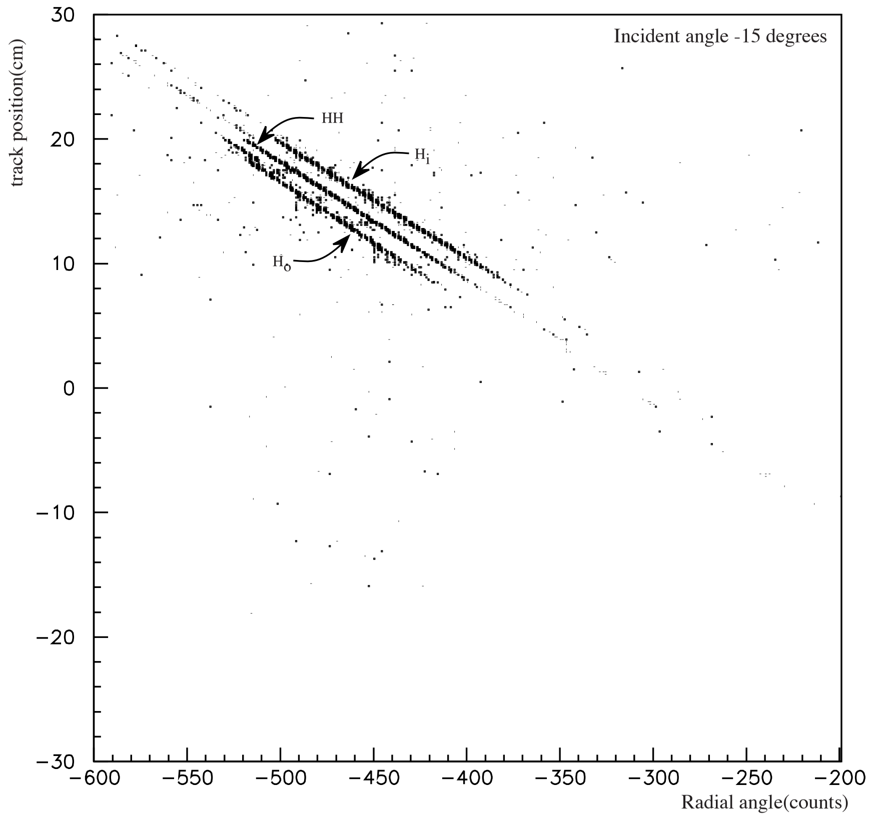

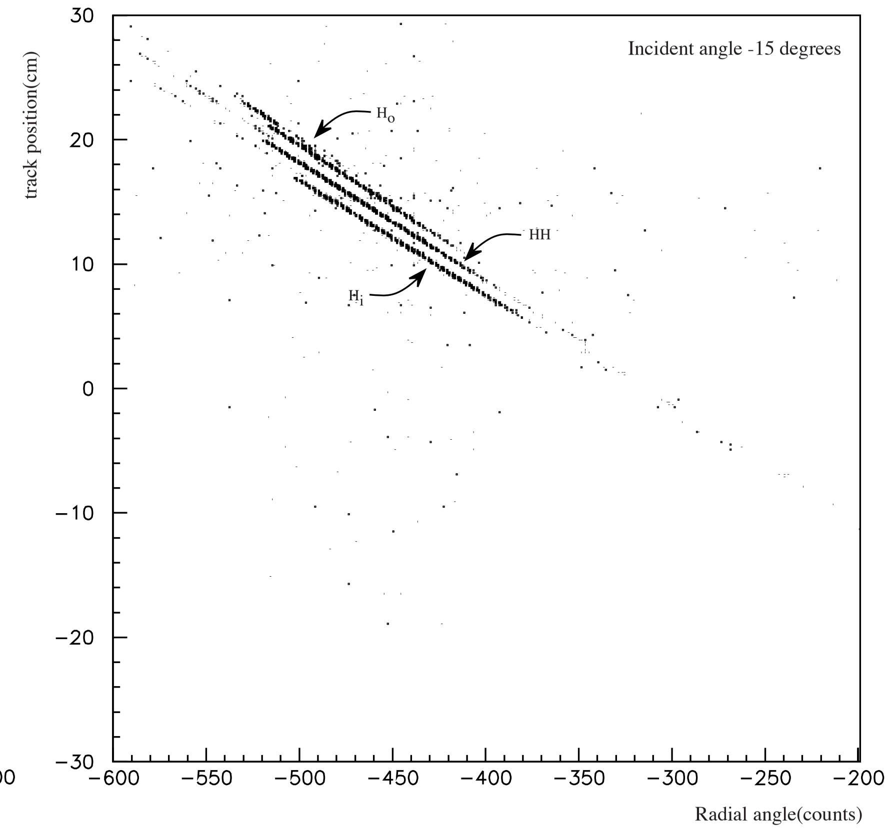

Figure 11- Correlation between crossing coordinate measured from a track fit and radial angle as output from the trigger at correct clock before extrapolation (left) and after extrapolation (right.)

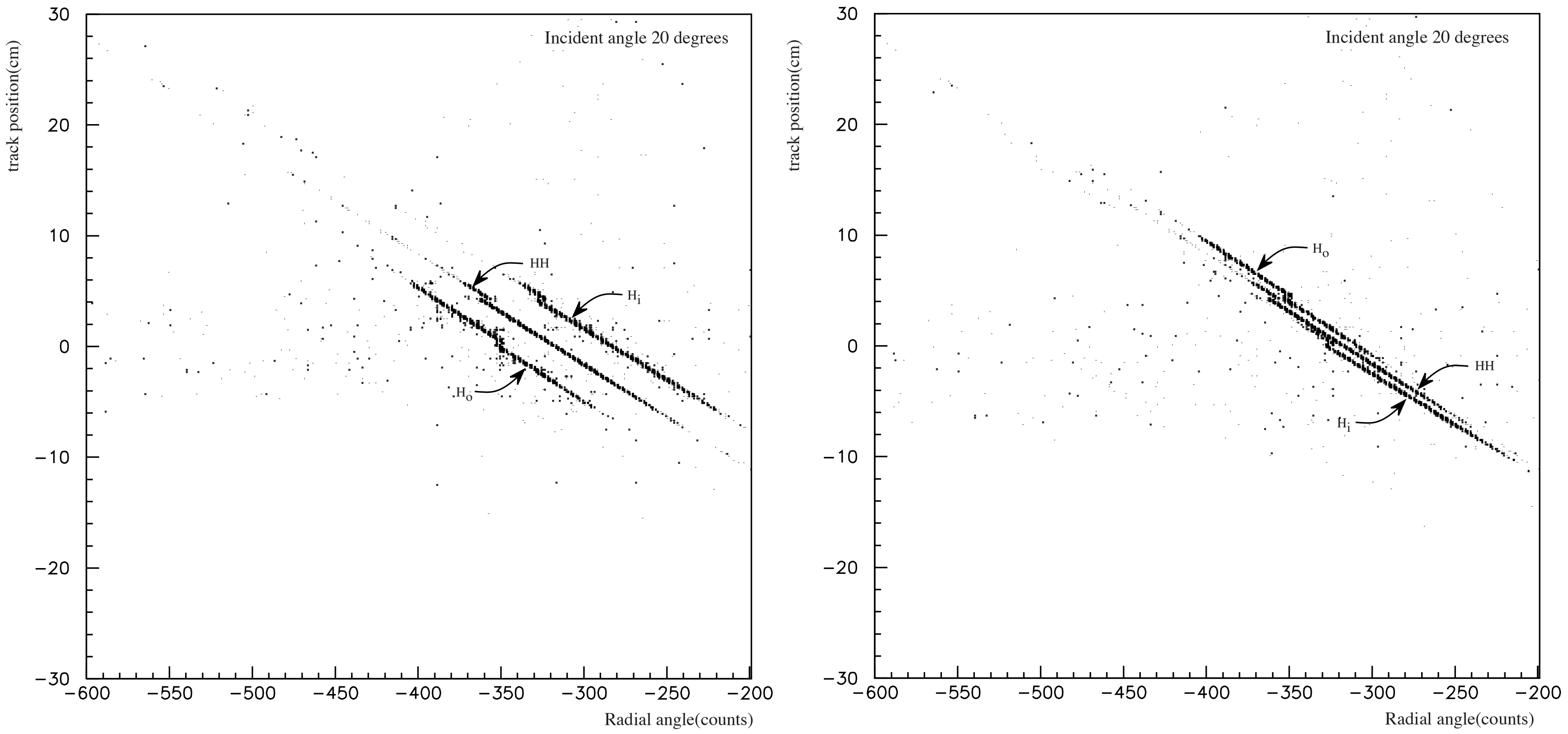

Figure 12- Correlation between crossing coordinate measured from a track fit and radial angle as output from the trigger at correct clock before extrapolation (left) and after extrapolation (right.)

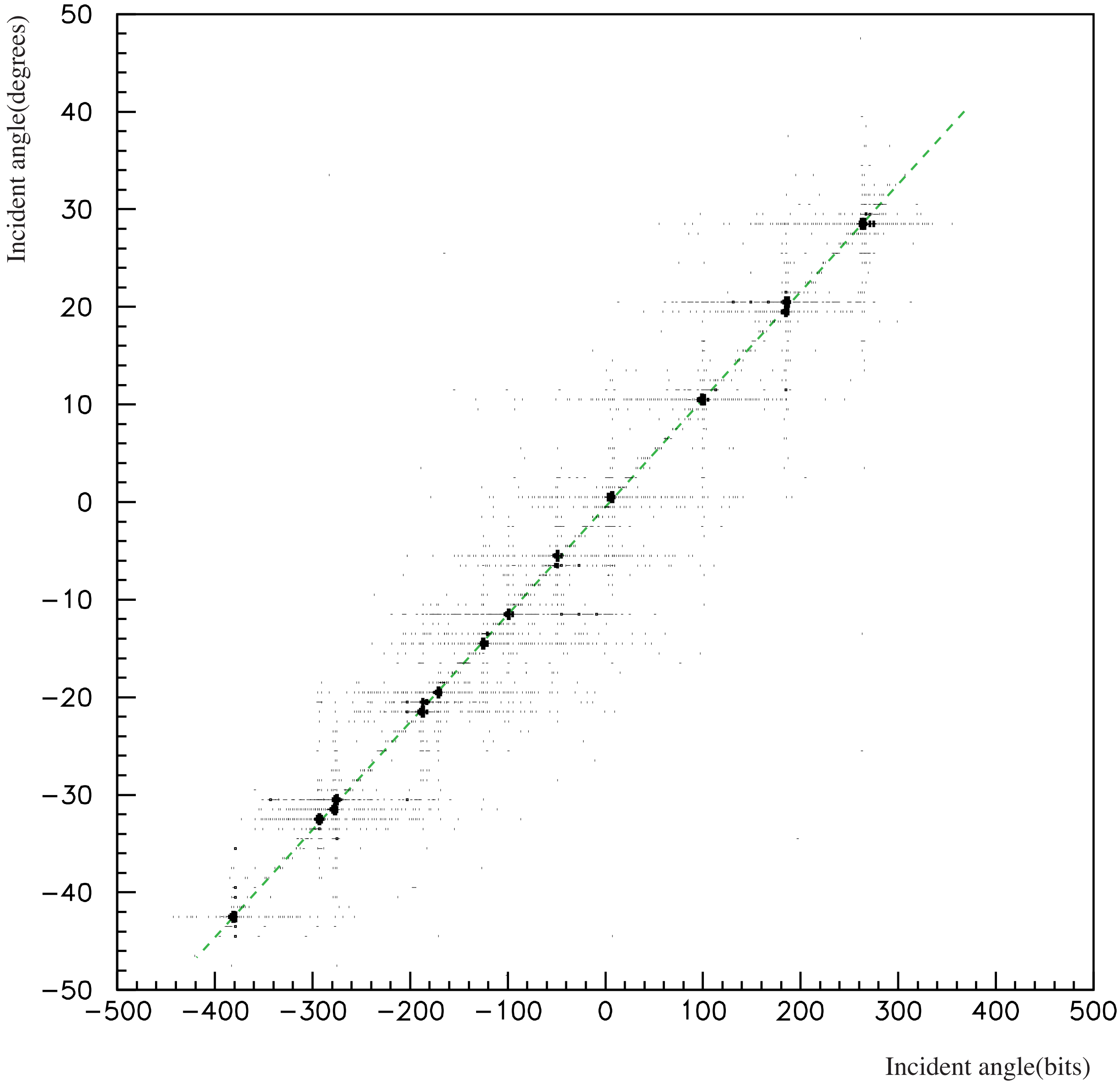

Figure 13- Correlation between incident angle as recorded from hardware data in TRACO units and incident angle as obtained form track fitting in degrees. The dashed line is drawn only to guide the eye.